Organic Process Research & Development **2006**, *10*, 109–117

Understanding the Origin of Unusual Stepwise Hydrogenation Kinetics in the Synthesis of the 3-(4-Fluorophenyl)morpholine Moiety of NK_1 Receptor Antagonist Aprepitant

Karel M. J. Brands,*,† Shane W. Krska,*,‡ Thorsten Rosner,*,‡ Karen M. Conrad,† Edward G. Corley,† Mahmoud Kaba,‡ Robert D. Larsen,† Robert A. Reamer,† Yongkui Sun,‡ and Fuh-Rong Tsay†

Departments of Process Research and Chemical Engineering Research and Development, Merck Research Laboratories, P.O. Box 2000, Rahway, New Jersey 07065, U.S.A.

Abstract:

An efficient and highly stereoselective one-pot Grignard addition/hydrogenation procedure is a key step in the synthesis of the NK_1 receptor antagonist aprepitant. The critical influence of pH on the nature and stability of the intermediate Grignard adducts, along with their reactivity in the hydrogenation reaction, is described. The observation of a defluorinated impurity under hydrogen-starved conditions led to mechanistic studies that revealed unusual kinetics in the hydrogenation reaction. Detailed analysis of the kinetic profiles under hydrogen-starved conditions indicated the two steps of the reaction, debenzylation of the Grignard adducts and reduction of the incipient imine, occurred in near perfect stepwise fashion wherein the debenzylation reaction was essentially complete before any imine reduction took place. Under hydrogen-saturated conditions the inhibition of the imine reduction was less complete, but the partial buildup of reactive imine intermediate led to a dramatic spike in reaction rate toward the end of reaction. Possible mechanistic rationales to explain these observation are discussed.

Introduction

The pharmacologic actions of the neuropeptide substance-P have been associated with conditions as diverse as inflammation,[1] emesis,[2] and CNS disorders.[3] This has prompted a search for small-molecule antagonists for the human neurokinin-1 (NK_1) receptor[4] to which substance-P preferentially binds.[5] Aprepitant (**1**),[6] a potent and orally active NK_1 antagonist, is the active ingredient in Emend

Scheme 1

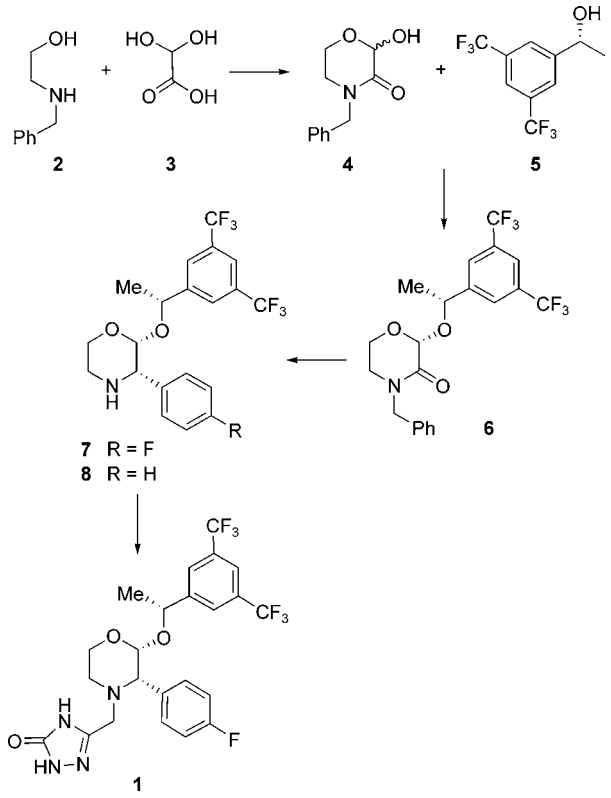

which is currently being marketed as a treatment for chemotherapy-induced nausea and vomiting.[7] We recently reported an efficient and practical synthesis of **1** in only four operations (Scheme 1).[8] In one of the key steps lactam **6** is stereoselectively converted to α-arylamine **7** via the addition

* To whom correspondence should be addressed. E-mail: jos_brands@merck.com; shane_krska@merck.com.

† Department of Process Research.

‡ Department of Chemical Engineering Research and Development.

(1) (a) Longmore, J.; Swain, C. J.; Hill, R. G. *Drugs News Perspect.* **1995**, *8*, 5−23. (b) Weisman, M. H.; Hagaman, C.; Yaksh, T. L.; Lotz, M. *Semin. Arthritis Rheum.* **1994**, *23*, 18−24. (c) Joos, G. F.; Germonpre, P. R.; Kips, J. C.; Peleman, R. A.; Pauwels, R. A. *Eur. Respir. J.* **1994**, *7*, 1161−1171. (d) Julia, V.; Morteau, O.; Bueno, L. *Gastroenterology* **1994**, *107*, 94−102.

(2) Andrews, P. L. R.; Rapeport, W. G.; Sanger, W. G. *Trends Pharmacol. Sci.* **1988**, *9*, 334−314.

(3) (a) Barker, R. *Neurosci. Rev.* **1996**, *7*, 187−214. (b) Longmore, J.; Hill, R. G.; Hargreaves, R. J. *Can. J. Phys.* **1997**, *75*, 612−621. (c) Teixeira, R. M.; Santos, A. R. S.; Ribeiro, S. J.; Calixto, J. B.; Rae, G. A.; De Lima, T. C. M. *Eur. J. Pharmacol.* **1996**, *311*, 7−14.

(4) Desai, M. C. *Expert Opin. Ther. Pat.* **1994**, *4*, 315−321 and references therein.

(5) Regoli, D.; Boudon, A.; Fauchere, J.-L. *Pharmacol. Rev.* **1994**, *46*, 551−599.

(6) (a) Hale, J. J.; Mills, S. G.; MacCoss, M.; Shah, S. K.; Qi, H.; Mathre, D. J.; Cascieri, M. A.; Sadowski, S.; Strader, C. D.; MacIntyre, D. E.; Metzger, J. E. *J. Med. Chem.* **1996**, *39*, 1760−1762. (b) Hale, J. J.; Mills, S. G.; MacCoss, M.; Finke, P. E.; Cascieri, M. A.; Sadowski, S.; Ber, E.; Chicci, G. G.; Kurtz, M.; Metzger, J.; Eierman, G.; Tsou, N. N.; Tattersall, F. D.; Rupniak, N. M. J.; Williams, A. R.; Rycroft, W.; Hargreaves, R.; MacIntyre, D. E. *J. Med. Chem.* **1998**, *41*, 4607−4614.

(7) (a) Kris, M. G.; Radford, J. E.; Pizzo, B. A.; Inabinet, R.; Hesketh, A.; Hesketh, P. J. *J. Natl. Cancer Inst.* **1997**, *89*, 817−818. (b) Rupniak, N. M. J.; Tatersall, F. D.; Williams, A. R.; Rycroft, W.; Carlson, E. J.; Cascieri, M. A.; Sadowski, S.; Ber, E.; Hale, J. J.; Mills, S. G.; MacCoss, M.; Seward, E.; Huscroft, I.; Owen, S.; Swain, C. J.; Hill, R. G.; Hargreaves, R. J. *Eur. J. Pharmacol.* **1997**, *326*, 201−209.

(8) Brands, K. M. J.; Payack, J. F.; Rosen, J. D.; Nelson, T. D.; Candelario, A.; Huffman, M.; Zhao, M. M.; Li, J.; Craig, B.; Song, Z. J.; Tschaen, D. M.; Hansen, K.; Devine, P. N.; Pye, P. J.; Rossen, K.; Dormer, P. G.; Reamer, R. A.; Welch, C. J.; Mathre, D. J.; Tsou, N. N.; McNamara, J. M.; Reider, P. J. *J. Am. Chem. Soc.* **2003**, *125*, 2129−2135.

10.1021/op0501895 CCC: $33.50
Published on Web 12/07/2005

Scheme 2

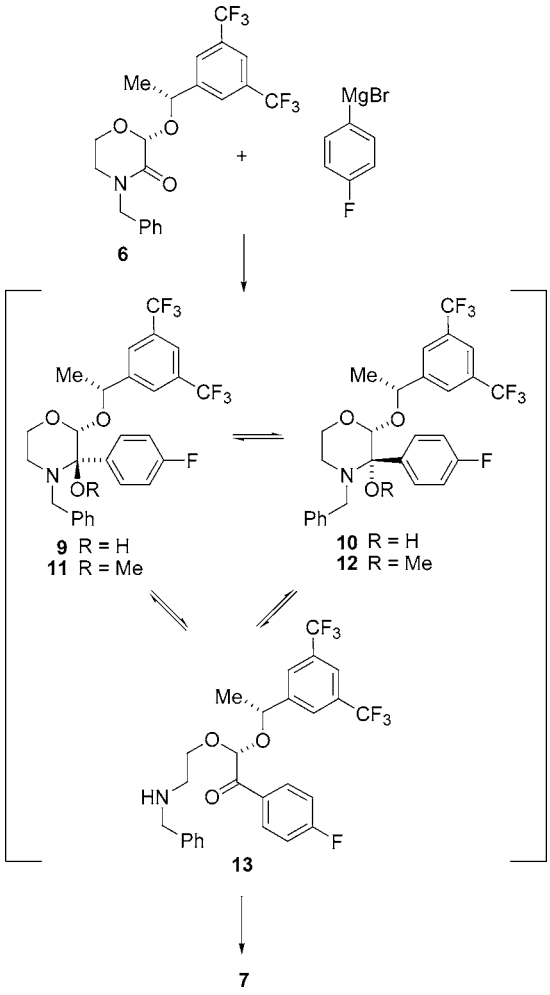

of a Grignard reagent followed by a quench and immediate hydrogenation. Under optimized conditions this operation provides **7** in 89−94% isolated yield as its hydrochloride salt. However, in initial scale-up of this chemistry unacceptable levels of defluorinated **8** were formed. This observation prompted a mechanistic study to understand the factors governing the selectivity of the hydrogenation. The results revealed significant insight into a rare example of stepwise kinetics in a heterogeneously catalyzed hydrogenation reaction.

Results and Discussion

Effect of Acid Charge. As illustrated in Scheme 2, the first step of the one-pot stereoselective conversion of *N*-benzyl lactam **6** into α-arylamine **7** involves the addition of 1.3 equiv of 4-fluorophenylmagnesium bromide in THF followed by a quench with methanol and acidification with 4-toluenesulfonic acid (*p*-TSA). This yields, according to NMR, an equilibrium mixture of five species whose relative proportions depend on the amount of added acid (Figure 1). Hemiaminal diastereomers **9** and **10** predominate at low equivalents of added acid, along with smaller amounts of aminals **11** and **12**. Each pair of diastereomers is present in a 2:1 ratio. The relative stereochemistry of the major and minor diastereomers cannot be unambiguously deduced from NMR. Ring-opened ketone **13**, which is presumably more

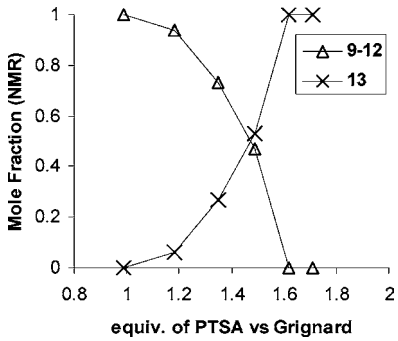

Figure 1. **Effect of acid/base stoichiometry on the composition of Grignard adducts 9−13 determined by ^{1}H NMR spectroscopy. Samples were prepared by reacting 6 with 1.30 equiv of 4-fluorophenylmagnesium bromide in THF at 20 °C, followed by a quench into MeOH and addition of the indicated amount of 4-toluenesulfonic acid (see Experimental Section).**

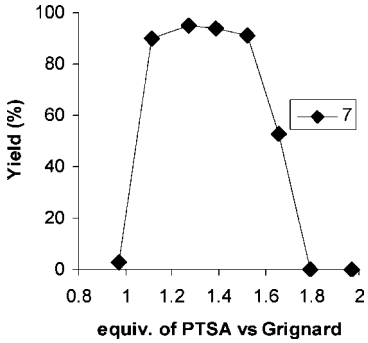

Figure 2. **Effect of acid/base stoichiometry on the hydrogenation yield of 7 (determined by HPLC). Reaction mixtures were prepared by reacting 6 with 1.30 equiv of 4-fluorophenylmagnesium bromide in THF at 20 °C, followed by a quench into MeOH and addition of indicated amount of 4-toluenesulfonic acid. Hydrogenations were carried out for 3 h at 22 °C and 5 psig of hydrogen in the presence of 5 wt % of a 5% Pd/C catalyst in a mixture of THF and MeOH.**

basic[9] than **9**−**12**, predominates at higher acid charges and is the exclusive species above 1.6 equiv.

In the second part of the one-pot conversion of **6** to **7** the above mixture of intermediates is hydrogenated over 5% Pd/C in a 1:1 mixture of MeOH and THF. Here the equivalency of added *p*-TSA exerts a profound influence on the rate and selectivity. As illustrated in Figure 2, when less than one equivalent of *p*-TSA is added relative to Grignard reagent, very little of **7** is produced after 3 h of reaction. While unreacted **9**−**13** constitute the majority of the end-of-reaction mixture in this case, small amounts (12 area % by HPLC) of *N*-benzyl *sec*-amine **14** are observed along with ring-opened amino-alcohols **15** and **16** which are presumably derived from reduction of **13** (Scheme 3). As the amount of acid increases, the yield of **7** also increases to a maximum of ∼95% at 1.3−1.4 equiv of *p*-TSA relative to the Grignard adduct, before it dramatically drops to zero when the amount of *p*-TSA exceeds 1.7 equiv. Under the latter conditions, the reaction mixture after 3 h only contains unconverted ring-opened ketone **13**. Interestingly, a reaction using 1.66 equiv of *p*-TSA gave only a 50% yield of **7**, with the balance

(9) Bell, R. P. In *Advances in Physical Organic Chemistry*; Gold, V., Ed.; Academic Press: New York, 1966; Vol 4, pp 1−29.

Scheme 3

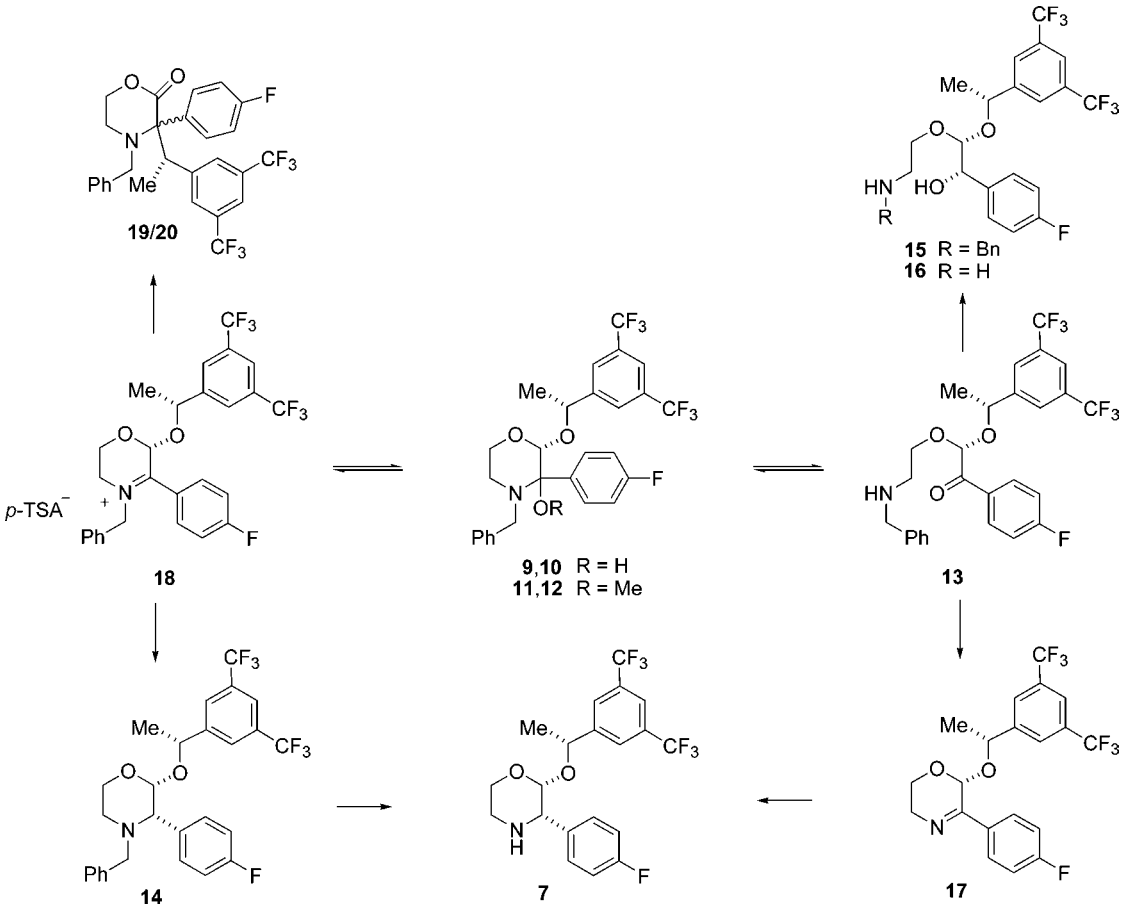

according to HPLC being imine **17** (Scheme 3). Imine **17** and *N*-benzyl *sec*-amine **14** are potential intermediates leading to the desired product **7**. As shown in Scheme 3, debenzylation of **9**−**13** followed by elimination of water or MeOH would give imine **17**; a second reduction, which can be expected to be highly stereoselective, would then lead to **7**. The observation of *N*-benzyl *sec*-amine **14** is likely the result of an initial stereoselective reduction of **18**. Debenzylation of **14** in a consecutive step would then also give **7**. Indeed, in a control experiment **14** provided **7** smoothly under the reaction conditions. Iminium **18** is also a likely intermediate in the previously described rearrangement[8] of **9**−**13** to a pair of lactone diastereomers **19** and **20**. Interestingly, the rate of this rearrangement reaches a maximum when 1.3−1.7 equiv of *p*-TSA are present relative to the Grignard reagent, mirroring the conditions where the maximum rate and selectivity occur in the hydrogenation reaction.

The performance of the hydrogenation reaction as a function of the *p*-TSA charge may be qualitatively rationalized as follows. Under overall basic conditions (i.e., <1.0 equiv of acid added relative to the Grignard reagent) the starting adducts are present largely as ring-closed aminals **9**−**12**. Formation of iminium salt **18** under these conditions is likely to be slow, impeding the rearrangement to **19**/**20**, or the hydrogenation to **14**. Direct *N*-debenzylation of **9**−**12** is presumably also slow under these basic conditions.[10] With all other reactions relatively slow, ketone reduction of **13** (present in low concentrations) can thus become competitive. In the presence of relatively small amounts of *p*-TSA (1.0−1.6 equiv relative to the Grignard reagent) the preequilibrium between **9**−**13** and **18** is established relatively fast. *N*-Debenzylation of **9**−**13** to yield **17** is now significantly faster than rearrangement to **19**/**20** or ketone reduction of **13** to **15**. In the presence of relatively large amounts of *p*-TSA (>1.6 equiv relative to the Grignard reagent) the starting material is largely present as ring-opened ketone **13** (in its protonated form). Debenzylation and ketone reduction of **13** under these conditions are apparently slow. The rearrangement to **19**/**20** does not occur either under these conditions because the equilibrium between **18** and **13** lies completely on the side of the latter.

After workup of a hydrogenation reaction performed under optimum conditions, **7** can be crystallized as its hydrochloride salt in 89−94% overall isolated yield with >350:1 diastereoselectivity at the newly formed stereogenic center and >99.7 area % purity according to HPLC analysis. This overall yield indicates that each step (one nucleophilic addition step and two reduction steps) occurs with >95% efficiency. However, when this procedure was first performed on multikilogram scale, the reaction required several more hours to reach completion and produced up to 0.5 area % of desfluoro **8** in the isolated solid. This impurity was not rejected in a recrystallization of **7**. It was established that the formation of **8** did not occur before the start of the

(10) Studer, M.; Blaser, H.-U. *J. Mol. Catal. A.* **1996**, *112*, 437−445 and references therein.

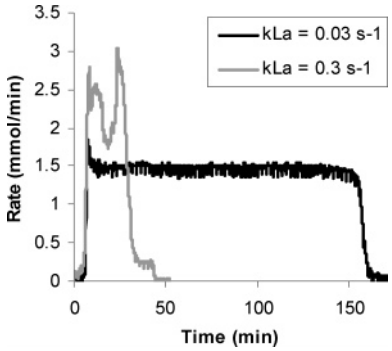

Figure 3. **Comparison of the rate of hydrogen uptake for hydrogenations using agitation rates of 500 and 1000 rpm (k_La = 0.03 and 0.3 s^{-1}, respectively). The substrate solution was prepared as outlined in the Experimental Section and then hydrogenated with 10 wt % of 5% Pd/C at 20.0 °C and 5 psig of H_2.**

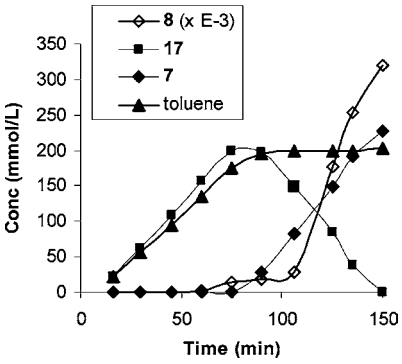

Figure 4. **Reaction profile of the hydrogenation performed at relatively low agitation (k_La = 0.03 s^{-1}). The hydrogenation was performed at 500 rpm agitation as described under Figure 3. Samples were taken, immediately filtered, diluted, and analyzed by LC−MS.**

hydrogenation as the 4-fluorophenylmagnesium bromide from the sources we used did not contain any phenylmagnesium bromide. In addition, the amount of **8** also did not increase significantly upon aging of the hydrogenation reaction mixture for an extended time. It was determined that, after the hydrogen uptake ceases, **8** grows at <0.01 area % h^{-1}. Therefore, an investigation was undertaken to determine the factors governing the defluorination reaction so that formation of **8** could be controlled at a more acceptable level (i.e., less than 0.1 area %).

Hydrogenation Kinetics and Formation of Desfluoro 8. The variable kinetics and formation of **8** which were observed when the above hydrogenation was performed on larger scale hinted at hydrogen mass transfer effects in this process. In hydrogenation reactions with fast intrinsic rates, the rate of hydrogen transport across the gas−liquid interface can become rate-limiting. In these cases, the steady-state solution concentration of hydrogen approaches zero, which can result in profound changes in selectivity.[11] Gas−liquid mass transfer is a first-order process (eq 1), with an overall rate governed by rate constant k_La and the difference between the actual and saturation solution concentrations of H_2 ($[H_2]$ and $[H_2]_{sat}$, respectively), the latter being a function of H_2 headspace pressure.[12] The k_La for a given reaction mixture varies strongly with the agitation speed, the vessel fill level and the geometry of the impeller and reactor.

$$\frac{d[H_2]}{dt} = k_L a([H_2]_{sat} - [H_2]) \quad (1)$$

To test the impact of mass transfer effects on the reaction, hydrogenations were performed with 10 wt % of 5% Pd/C catalyst at two different agitation rates under otherwise identical conditions (20 °C and 5 psig of H_2). Figure 3 shows the rates of hydrogen uptake for reactions at 500 and 1000 rpm, k_La = 0.03 and 0.3 s^{-1}, respectively.

The marked effect of stirring on the reaction rate indicates that the reaction is operating under hydrogen diffusion limitations at lower k_La values. In accord with this, the reaction conducted at 500 rpm exhibits kinetics which are apparently zero order in substrate, a consequence of the rate-limiting step being hydrogen mass transfer (which is zero order in [substrate], and pseudo-zero order in $[H_2]$ due to constant headspace pressure).[13] More importantly, the amounts of desfluoro **8** in the isolated solids were 0.23 and 0.02 area % for the 500 and 1000 rpm reactions, respectively.

The reaction with k_La 0.03 s^{-1} was repeated and sampled at regular intervals with the results shown in Figure 4. Only traces of *N*-Bn-*sec*-amine **14** were observed throughout the course of the reaction, implying that this intermediate is not likely on the primary pathway to **7**. Instead, imine intermediate **17** is observed in ∼90% assay yield at the midpoint of the reaction. The linear shape of the profiles for **7**, **17**, and toluene in Figure 4 are a consequence of the zero-order kinetics imposed by the hydrogen mass transfer limitation. Since the reaction that forms **8** is 3 orders of magnitude slower than the other processes, its intrinsic kinetics are not masked by mass transfer effects, and therefore the profile of **8** exhibits a sigmoidal shape. The most surprising feature of the profiles in Figure 4 is that it appears that the reaction occurs in near perfect stepwise fashion. In the first half of the reaction the Grignard adduct mixture of **9**−**13** is debenzylated to provide imine **17** (and toluene). At the midpoint of the hydrogen uptake, the debenzylation is complete (as is evidenced by the leveling off in toluene concentration), and the accumulated imine intermediate **17** starts being reduced to morpholine **7**. It is at this point that the formation of defluorinated **8** also starts to occur. It is apparent that almost none of imine **17** is reduced to **7** before the starting Grignard adduct mixture is completely debenzylated.

To understand the reason for this unusual kinetic behavior, it was necessary to observe the underlying kinetics of the

(11) For examples, see: (a) Singh, U.K.; Landau, R. N.; Sun, Y.; LeBlond, C.; Blackmond, D. G.; Tanielyan, S. K.; Augustine, R. L. *J. Catal.* **1995**, *154*, 91−97. (b) Sun, Y.; Landau, R. N.; Wang, J.; LeBlond, C.; Blackmond, D. G. *J. Am. Chem. Soc.* **1996**, *118*, 1348−1353.

(12) For a useful discussion of k_La, including experimental techniques for its measurement, see: Deimling, A.; Karandikar, B. M.; Shah, Y. T. *Chem. Eng. J.* **1984**, *29*, 127−140.

(13) Further support for the reaction rate being mass transfer limited comes from the close agreement between the observed H_2 uptake rate (5.5×10^{-5} M/s) and the maximum H_2 delivery rate (6.0×10^{-5} M/s) calculated from eq 1 assuming $[H_2] = 0$, and using experimentally determined values of k_La = 0.03 s^{-1} and $[H_2]_{sat} = 2.0 \times 10^{-3}$ M.

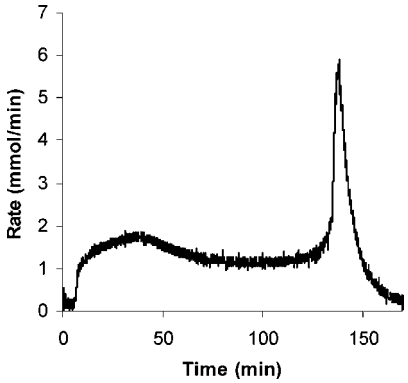

Figure 5. **Hydrogen uptake rate profile for a typical hydrogenation reaction conducted under non-mass-transfer-limited conditions. Substrate solution (425 mL), prepared as described in the Experimental Section, was hydrogenated in the presence of 2 wt % of 5% Pd/C at 20 °C, 20 psig of H_2 and 2000 rpm ($k_La = 2.7\ s^{-1}$).**

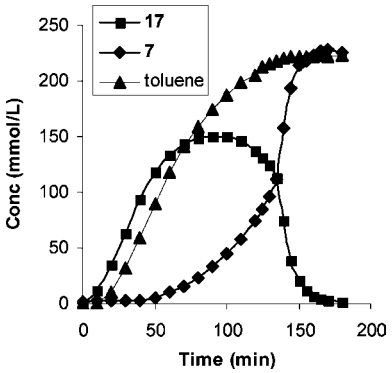

Figure 6. **Profile determined by LC−MS analysis of reaction samples for a typical hydrogenation conducted under non-mass-transfer-limited conditions. Substrate solution (425 mL) prepared as described in the Experimental Section was hydrogenated in the presence of 2 wt % of 5% Pd/C at 20 °C, 20 psig of H_2 and 2000 rpm ($k_La = 2.7\ s^{-1}$). Samples were taken, immediately filtered, diluted, and analyzed by LC−MS.**

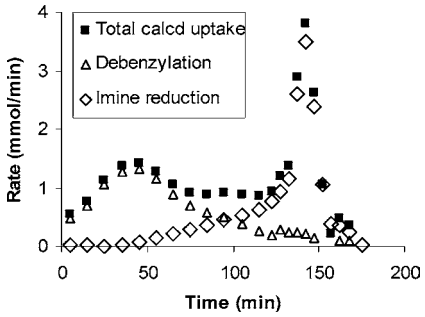

Figure 7. **Instantaneous rate profiles of debenzylation and imine reduction calculated from the first derivatives of LC−MS concentration profiles shown in Figure 6.**

hydrogenation free from the distortions caused by mass transfer effects. This was accomplished by increasing the rate of hydrogen mass transfer (through faster agitation and higher hydrogen pressure) and reducing the intrinsic rate of the hydrogenation (by lowering the catalyst loading) such that the maximum hydrogen mass transfer rate, $k_La[H_2]_{sat}$, was at least 10 times faster than the maximum intrinsic reaction rate. Under these conditions, the reaction mixture was expected to be nearly saturated in hydrogen throughout the course of the reaction ($[H_2]_{sat} \approx 5$ mM at 20 psig). Reactions were run in a Mettler Toledo RC1 reaction calorimeter and followed by hydrogen uptake, calorimetry, and LC−MS analysis of samples. Figure 5 shows the first derivative of the hydrogen uptake profile for a typical reaction. The instantaneous rate profile shown in this plot matches well with that derived from the measured heat-flow.

The rate profile of the hydrogenation reaction shown in Figure 5 exhibits some unusual features. After an initial activation period, the rate steadily increases until a maximum is reached after approximately 40 min. The rate then slightly decreases before it settles into apparent zero-order behavior. However, when the reaction reaches ~70% of the total theoretical hydrogen uptake, there is a sudden 4-fold acceleration in the rate followed by a nearly pure first-order decay to zero. The observed first-order rate constant for this latter regime had a value of $k_{obs} = 2.1 \pm 0.1 \times 10^{-3}\ s^{-1}$ (using 2 wt % of 5% Pd/C at 20 °C) and was found to be independent of hydrogen pressure over the range of 20−70 psig.

Monitoring the progress of the reaction by taking samples and analyzing them by LC−MS afforded the profiles shown in Figure 6. As before, *N*-Bn-*sec*-amine **14** was only a minor component (<5 mol %) in all samples tested; desfluoro impurity **8** was not detected in any of the samples. Although there still is significant buildup of imine **17**, the reaction under these conditions is no longer purely sequential. The point at which the reaction undergoes a sudden acceleration is clearly reflected in the changing slopes of the imine and product curves at approximately 135 min. A more instructive way to look at the data in Figure 6 is to plot the first derivative of the concentration profiles to visualize how the instantaneous rates of debenzylation and imine reduction contribute to the overall rate of hydrogen uptake (Figure 7). This analysis shows that each of the two reactions exhibits a characteristic curved rate profile. That of the debenzylation reaction is broad, peaking early in the reaction before slowly tailing off. The rate profile of the imine reduction shows a long, gradual acceleration leading to the eventual rate spike, followed by a rapid denouement. In the regime between these respective rate maxima, the steadily increasing rate of imine hydrogenation compensates for the decreasing rate of debenzylation, thus giving rise to the apparent zero-order kinetics.

The unusual kinetic behavior exhibited by this reaction raises several intriguing mechanistic questions: Why are the two hydrogenation steps (debenzylation and imine reduction) perfectly sequential under mass transfer limited conditions, and only partially sequential when run saturated in hydrogen? Why is the apparently faster-reacting species (the imine) hydrogenated at a slower observed rate than the Grignard adduct for most of the course of the reaction under both hydrogen-saturated and -starved conditions? Which mechanistic factors can account for the sudden spike in rate seen in Figures 5−7?

Mechanistic Rationale for Stepwise Kinetics. Hydrogenations using supported heterogeneous catalysts exhibit characteristic kinetic behavior arising from the involvement

of multiple adjacent catalytic sites in elementary reaction steps and competition between substrate(s) and hydrogen for active catalyst sites.[14] Recently Rousseau and co-workers reported that hydrodehalogenations of aryl iodides in the presence of substituted alkenes occur in a perfectly stepwise manner, in which the more slowly reacting aryl iodide must be completely consumed before hydrogenation of the alkene will commence.[15] The resulting concentration profiles of aryl iodide and alkene bear a striking resemblance to the profiles shown in Figure 4. The mechanistic hypothesis put forth by Rousseau and co-workers to explain their observations involves competition for active catalyst sites between the aryl iodide and alkene, with the more strongly binding aryl iodide effectively displacing the alkene from the catalyst surface until it is completely consumed by the hydrodehalogenation reaction, at which point the hydrogenation of the alkene is allowed to commence.

The obvious similarity between Rousseau's observations and our own led us to consider a similar mechanism. Thus, one might hypothesize that the Grignard adduct (or mixture of rapidly equilibrating adducts) is strongly bound to the catalyst surface but is relatively slowly hydrogenated. In contrast, the intrinsic hydrogenation rate of the resulting imine intermediate is relatively fast, but the binding of this species to the catalyst could be relatively weak. Certainly, the curves shown in Figure 4 would be consistent with this hypothesis. However, such a simple mechanism cannot account for the kinetics shown in Figures 5−7. Under hydrogen-saturated conditions the two reactions (debenzylation and imine reduction) are no longer purely sequential, since significant imine hydrogenation (approximately 30%) takes place *prior* to the rate spike seen at the end of the reaction. The relative binding strengths of Grignard adduct and imine would not be expected to change based upon the solution concentration of hydrogen. Thus, it seemed likely that competitive binding of hydrogen was also an important factor in determining the overall observed kinetics.

In this regard, Hawkins, Blackmond and co-workers recently reported a kinetic study of the hydrogenation of a substituted nitrobenzene derivative over Pd/C that exhibited an extended zero-order regime followed by a sudden rate acceleration.[16] In contrast to the present system, no intermediates were observed in this reaction. The unusual kinetic profile was modelled by invoking balancing rates of two simultaneous catalytic pathways: the pathway that dominates at earlier reaction times involves substrate reacting with hydrogen at a single catalytic site in the rate-determining step (the Rideal mechanism); at later reaction times the second pathway, involving substrate and hydrogen activation at two adjacent catalytic sites (the Langmuir−Hinshelwood mechanism), becomes dominant. The latter pathway exhibits a negative reaction order in [substrate] until the optimal ratio of substrate and hydrogen surface coverage is reached, followed by a rapid deceleration as substrate is depleted, thus accounting for the rate spike seen at the end of the reaction.

Extending these ideas to the present system, one can construct a simple kinetic model based on the Langmuir−Hinshelwood mechanism involving simultaneous binding of Grignard adduct **9**−**13** (treated as one species), imine **17**, and hydrogen. Assuming strong binding of Grignard adduct relative to imine and a faster rate of imine reduction relative to Grignard adduct and neglecting the catalyst activation period at the beginning of the reaction, this simple model can reproduce the spike seen in the rate of the imine reduction near the end of the reaction under hydrogen-saturated conditions. However, the model fails to reproduce the rate profile for the debenzylation step, incorrectly predicting quasi-zero-order kinetics for this process throughout the beginning of the reaction, followed by a sudden drop-off in rate concomitant with the imine reduction spike. In addition, this simple model cannot account for the observed kinetics under mass transfer limited conditions.

Clearly, the complex kinetics of this system defy explanation by simple models based upon quasi-equilibrium assumptions. It is likely that nonsteady-state effects arising from the many competing rate processes present in this system are responsible for the observed features of the rate profile. For example, one could imagine that the Grignard adduct actually reacts more quickly with surface-bound hydrogen than the imine, effectively inhibiting the reduction of the latter by scavenging all available activated hydrogen. This type of inhibition, in contrast to the Rousseau results described above, would arise from kinetic, rather than thermodynamic, effects. If this were indeed the case, one would have to postulate that some other step prior to the Grignard adduct debenzylation, for example binding and activation of hydrogen on the catalyst surface, would have to be rate-limiting in order to explain the relatively low observed rate of debenzylation of the Grignard adduct. In this scenario, once the Grignard adduct is mostly consumed, the nature of the catalyst surface would fundamentally change, becoming increasingly hydrogen-rich and favorable to imine reduction, thus resulting in the dramatic rate acceleration observed toward the end of the reaction under hydrogen-saturated conditions. This mechanistic picture could also rationalize the effects seen under mass transfer limited conditions, since starving the system of hydrogen would enhance this kinetic inhibition of the imine reduction, even at very low concentrations of Grignard adduct. In the end, it would be very difficult to empirically support such a mechanistic postulate,[17] and doubtless other possible explanations exist. Nevertheless, the foregoing discussion offers an intriguing possibility that differs significantly from conventional kinetic treatments of such systems.

(14) Augustine, R. L. *Heterogeneous Catalysis for the Synthetic Chemist*; Marcel Dekker: New York, 1996.

(15) (a) Ambroise, Y.; Mioskowski, C.; Djéga-Mariadassou, G.; Rousseau, B. *J. Org. Chem.* **2000**, *65*, 7183−7186. (b) Faucher, N.; Ambroise, Y.; Cintrat, J.-C.; Doris, E.; Pillon, F.; Rousseau, B. *J. Org. Chem.* **2002**, *67*, 932−934.

(16) LeBars, J.; Dini, S.; Hawkins, J. M.; Blackmond, D. G. *Adv. Synth. Catal.* **2004**, *346*, 943−946.

(17) A kinetic model constructed from all the presumed elementary steps of the catalytic reaction was successfully fit in dynamic fashion to the experimental data under both hydrogen-saturated and -starved conditions. The qualitative picture arising from this model supports the speculative mechanistic hypothesis described in this paragraph. However, the model had too many adjustable parameters and was an over-determined system and, thus, could not be considered as strong support for this mechanism.

Scheme 4

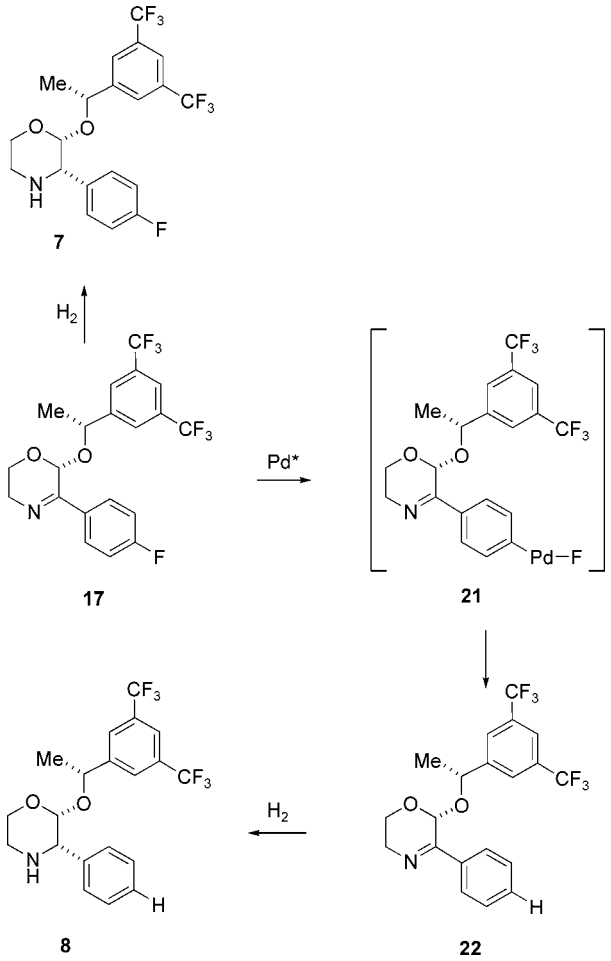

Reducing the Formation of Desfluoro Compound 8. Our better understanding of the intricate kinetic behavior of the hydrogenation reaction did not necessarily address the question of how **8** is formed and why its formation is favored at low hydrogen pressure and k_La. Scheme 4 provides a simple working hypothesis.[18] Rate-limiting oxidative insertion of active palladium zero into the carbon−fluorine bond of imine **17** (which is presumably further activated by protonation or complexation with magnesium under the reaction conditions) provides intermediate **21**. Reaction of the latter with surface-bound hydrogen yields the defluorinated imine **22** which is further reduced to **8** at a rate similar to that of the reduction of **17** to **7**.[19] According to this proposal, the hydrodehalogenation of **17** is in competition with reduction to **7**. Under mass transfer limited conditions, the rate of the latter reduction decreases to the rate of hydrogen mass transfer. However, the hydrodehalogenation which is intrinsically much slower is not subject to this limitation and continues at the same rate. The net effect is a longer residence time for **17** in the reactor and a correspondingly higher level of **8**.

(18) It is important to note that alternative mechanistic explanations cannot be excluded on the basis of our data.

(19) A closely related type of defluorination was found in the patent literature. The high-yielding and selective 4-defluorination of 2,3,4,5,6-tetrafluorobenzoic acid with Pd/C in aqueous base has been reported by Nauman, K.; Ziemann, H. U.S. Patent 4,822,912; *Chem. Abstr.* **1989**, *110*, 23543.

On the basis of the above hypothesis the hydrogenation procedure was adjusted in three ways for further scale-up: (1) the catalyst loading was reduced from 10−15 to 3−6 wt %; (2) the concentration of dissolved hydrogen was increased by increasing the hydrogen pressure from 5 to 20 psig; (3) the gas−liquid mass transfer rate was increased by optimization of the agitator configuration and maximizing the agitation rate. Each of these factors was independently shown to diminish the levels of **8** formed in the reaction. In combination, formation of **8** was reduced to a nondetectable level.

Conclusions

An efficient and highly stereoselective one-pot procedure for the unprecedented conversion of an *N*-benzyl-lactam to an α-aryl-*sec*-amine was developed. Addition of 4-fluorophenylmagnesium bromide to *N*-benzyl-1,4-oxazin-3-one **6** followed by immediate hydrogenation of the resulting mixture of intermediates yielded 3-(4-fluorophenyl)morpholine derivative **7** which could be isolated as its hydrochloride salt in 89−94% overall yield. The structure and stability of the intermediate Grignard adducts and the selectivity of their reduction as a function of the pH was elucidated. Kinetic studies on the hydrogenation reaction provided valuable insight into the mechanism of this reaction under both hydrogen-saturated and hydrogen-starved conditions. Finally, it was unequivocally demonstrated that an undesired defluorination only occurs under hydrogen-starved conditions. Appropriate adjustment of the reaction conditions on the basis of a simple mechanistic hypothesis resulted in the control of the formation of the undesired impurity **8** at a nondetectable level.

Experimental Section

General. All commercially available reagents and solvents were used as received. Melting points are uncorrected. Elemental analyses were performed at Quantitative Technologies Inc., Whitehouse, NJ. NMR spectra were recorded on Bruker DPX-400 and DRX-600 spectrometers. The syntheses of reference samples for compounds **8** and **14** were not optimized. The preparation of **6** and the isolation and/or synthesis of authentic samples for compounds **15**−**17**, **19**, and **20** has been disclosed previously.[8]

[2*R*-[2α(*R),3α]]-2-[1-[3,5-Bis(trifluoromethyl)phenyl]-ethoxy]-3-(4-fluorophenyl)morpholine Hydrochloride (7·HCl).** To a solution of **6** (49.5 g; 110.6 mmol) in THF (50 mL) cooled to 15 °C was slowly added a solution of 4-fluorophenylmagnesium bromide in THF (0.99 M; 150 mL; 148.2 mmol) at such a rate that the temperature was maintained within 20−25 °C. The reaction mixture was stirred for another 30 min and then slowly added into ice-cold methanol (100 mL) at such a rate that the temperature was maintained between 0 and 10 °C. A solution of 4-toluenesulfonic acid (42.1 g; 221.3 mmol) in methanol (50 mL) was added followed by wet 5% Pd/C (45.5 wt % dry; 5.4 g). The resulting mixture was hydrogenated at 20−25 °C under 20 psi of hydrogen for 3 h. The slurry was filtered through cellulose. The filter bed was washed with methanol

(150 mL). The combined filtrates were evaporated to dryness and then partitioned between 4-methyl-2-pentanone (350 mL) and a solution of sodium bicarbonate (35.1 g) and sodium citrate dihydrate (42.0 g) in water (500 mL). The organic layer was separated, and concentrated hydrochloric acid (37.0 wt %; 13.0 g) was added. The resulting solution was distilled at atmospheric pressure until the total volume had reached approximately 200 mL and the product started to crystallize. The crystal slurry was allowed to cool to room temperature (RT) over a period of 3 h and then filtered. The solids were filtered, washed with 4-methyl-2-pentanone (2 × 50 mL), and dried at 75 °C in vacuo, yielding 47.6 g of the product (91% overall yield): mp 250 °C dec; $[\alpha]^{25}_{D} = +78°$ (c = 1.12, methanol); $[\alpha]^{25}_{365} = +217°$ (c = 1.12, methanol); ^{1}H NMR (400 MHz, $CDCl_3$) δ 10.82 (m, 1H), 10.47 (m, 1H), 7.65 (s, 1H), 7.59 (m, 2H), 7.21 (s, 2H), 7.05 (m, 2H), 4.91 (q, J = 6.6 Hz, 1H), 4.49 (m, 2H), 4.23 (d, J = 11.8 Hz, 1H), 3.81 (dd, J = 12.5, 3.7 Hz, 1H), 3.45 (m, 1H), 3.23 (m, 1H), 1.58 (d, J = 6.6 Hz, 1H). ^{13}C NMR (100 MHz, $CDCl_3$) δ 163.3 (d, J = 250.4 Hz), 144.1, 131.8 (q, J = 33.5 Hz), 129.9 (d, J = 8.3 Hz), 127.2 (d, J = 3.2 Hz), 126.1, 122.8 (q, J = 272.8 Hz), 121.8 (sep, J = 3.6 Hz), 116.0 (d, J = 22.0 Hz), 92.9, 72.9, 60.5, 55.1, 43.9, 24.1; Anal. Calcd for $C_{20}H_{19}ClF_7NO_2$: C, 50.70; H, 4.04; Cl, 7.48; F, 28.07; N, 2.96. Found: C, 50.34; H, 3.89; Cl, 7.55; F, 28.20; N, 2.79.

[2*R*-[2α(*R),3α]]-2-[1-[3,5-Bis(trifluoromethyl)phenyl]-ethoxy]-3-phenylmorpholine Hydrochloride (8·HCl).** To a solution of **6** (18.75 g; 41.9 mmol) in THF (20 mL) cooled to 15 °C was slowly added a solution of phenylmagnesium bromide in THF (1.0 M; 53 mL; 53.0 mmol) at such a rate that the temperature was maintained within 20−25 °C (10 min). The reaction mixture was stirred for another 30 min and then slowly added into ice-cold methanol (40 mL) at such a rate that the temperature was maintained below 10 °C. The reaction flask was rinsed with THF (10 mL). A solution of 4-toluenesulfonic acid (14.35 g; 75.4 mmol) in methanol (30 mL) was added followed by wet 5% Pd/C (45.5 wt % dry; 2.55 g). The resulting mixture was hydrogenated under 5 psi of hydrogen at 30 °C for 4 h and then at 35 °C overnight. The slurry was filtered through cellulose. The filter bed was washed with methanol (75 mL). The combined filtrates were evaporated to dryness and then partitioned between 4-methyl-2-pentanone (130 mL) and a solution of sodium bicarbonate (13.38 g) and sodium citrate dihydrate (14.78 g) in water (180 mL). The organic layer was separated and concentrated to dryness. The oily residue was filtered over a short plug of silica gel, eluting with a 4:1 mixture of ethyl acetate/hexane followed by ethyl acetate. The product fractions were combined and concentrated to dryness, yielding 9.3 of **8** (53% yield). This product was dissolved in 4-methyl-2-pentanone (120 mL), and concentrated hydrochloric acid (37.0 wt %; 2.21 g; 22.4 mmol) was added. The resulting solution was distilled at atmospheric pressure until the total volume had reached approximately 50 mL. Upon cooling, the product crystallized. The crystal slurry was allowed to cool to 5 °C over a period of 4 h and then filtered. The solids were filtered, washed with 4-methyl-2-pentanone, and dried at RT in vacuo, yielding 7.37 g of the product (39% overall isolated yield): mp 232 °C dec; $[\alpha]^{25}_{D} = +86$ (c = 2.66, methanol); $[\alpha]^{25}_{365} = +235$ (c = 2.66, methanol); ^{1}H NMR (600 MHz, $CDCl_3$) δ 10.86 (br d, J = 9.8 Hz, 1H), 10.49 (br q, J = 10.6 Hz, 1H), 7.64 (s, 1H), 7.53 (d, J = 7.6 Hz, 2H), 7.42 (t, J = 7.6 Hz, 1H), 7.36 (t, J = 7.6 Hz, 2H), 7.20 (s, 2H), 4.92 (q, J = 6.4 Hz, 1H), 4.57−4.52 (m, 1H), 4.55 (d, J = 1.5 Hz, 1H), 4.26 (d, J = 11.3 Hz, 1H), 3.83 (dd, J = 12.5, 3.8 Hz, 1H), 3.52 (br d, J = 12.5 Hz, 1H), 3.28−3.22 (m, 1H), 1.59 (d, J = 6.4 Hz, 3H). ^{13}C NMR (150 MHz, $CDCl_3$) δ 144.5, 132.1 (q, J = 33.6 Hz), 131.6, 129.8, 129.3, 127.9, 126.5 (q, J = 3.7 Hz), 123.1 (q, J = 272.8 Hz), 122.0 (m), 93.4, 73.1, 61.5, 55.6, 44.3, 24.5; Anal. Calcd for $C_{20}H_{20}ClF_6NO_2$: C, 52.70; H, 4.42; Cl, 7.78; F, 25.01; N, 3.07. Found: C, 52.61; H, 4.32; Cl, 7.71; F, 25.12; N, 2.98.

[2*R*-[2α(*R),3α]]-*N*-Benzyl-2-[1-[3,5-bis(trifluoromethyl)phenyl]ethoxy]-3-(4-fluorophenyl)morpholine Hydrochloride (14·HCl).** To a solution of **7**·HCl (20.0 g; 42.2 mmol) in DMF (100 mL) was added benzyl bromide (98%; 7.94 g; 45.5 mmol) and potassium carbonate (7.29 g; 52.7 mmol). The resulting slurry was stirred at RT overnight. 4-Methyl-2-pentanone (350 mL) and saturated sodium bicarbonate solution (600 mL) were added to the reaction mixture. The organic layer was separated, washed with saturated sodium bicarbonate solution (2 × 100 mL) and water (100 mL), and then concentrated hydrochloric acid (36.8 wt %; 5.02 g; 50.7 mmol) was added. The resulting slurry was distilled at atmospheric pressure until the total volume had reached approximately 100 mL. Upon cooling to RT, the solids were filtered, washed with 4-methyl-2-pentanone (2 × 50 mL), and dried at RT in vacuo, yielding 21.57 g of product (91% overall isolated yield): mp 209 °C dec; $[\alpha]^{25}_{D} = +82$ (c = 2.00, methanol); $[\alpha]^{25}_{365} = +247$ (c = 2.00, methanol); ^{1}H NMR (600 MHz, $CDCl_3$) δ 13.59 (br s, 1H), 7.65 (s, 1H), 7.47 (t, J = 7.6 Hz, 1H), 7.40 (t, J = 7.6 Hz, 2H), 7.16 (s, 2H), (d, J = 7.6 Hz, 2H), 4.89 (q, J = 6.4 Hz, 1H), 4.88−4.83 (m, 1H), 4.44 (d, J = 2.6 Hz, 1H), 4.36 (d, J = 14.0 Hz, 1H), 4.26 (d, J = 14.0 Hz, 1H), 3.96 (br s, 1H), 3.79 (dd, J = 12.5, 3.4 Hz, 1H), 3.59 (d, J = 11.7, 1H), 3.01 (br t, J = 11.0 Hz, 1H), 1.68 (d, J = 6.4 Hz, 3H); resonances from the *p*-fluorophenyl protons are extremely broad due to restricted rotation. ^{13}C NMR (150 MHz, $CDCl_3$) δ 163.8 (d, J = 252.1 Hz), 144.4, 132.3, 132.1 (q, J = 33.6 Hz), 130.8, 129.5, 126.4 (q, J = 4.3 Hz), 126.0 (d, J = 3.7 Hz), 123.1 (q, J = 272.8 Hz), 122.1 (m), 117. l (br), 93.7, 73.2, 65.9, 56.9, 56.3, 50.4, 24.5; resonances from the *p*-fluorophenyl methines are extremely broad due to restricted rotation; Anal. Calcd for $C_{27}H_{25}ClF_7NO_2$: C, 57.50; H, 4.47; Cl, 6.29; F, 23.58; N, 2.48. Found: C, 57.45; H, 4.26; Cl, 6.26; F, 23.72; N, 2.36.

Determination of Grignard Adduct Species Distribution (13 vs 9−12) as a Function of the Amount of 4-Toluenesulfonic Acid (Figure 1). To a solution of **6** (2.50 g; 5.58 mmol) in THF (3.0 mL) was added a solution of 4-fluorophenylmagnesium bromide in THF (freshly titrated to contain 0.99 M of active Grignard reagent and 1.0 M of total base; 7.50 mL; 7.41 mmol) between 20 and 25 °C. The

resulting solution was stirred at RT for 1 h and then cooled to −40 °C before methanol (7.50 mL) was added slowly. The resulting slurry was allowed to warm to RT, and 4-toluenesulfonic acid monohydrate (1.41 g; 7.41 mmol) was added in one portion. The resulting clear solution was transferred to a volumetric flask, and the volume was adjusted to 25.0 mL. A solution of 4-toluenesulfonic acid monohydrate (5.00 g) in methanol was prepared in a volumetric flask (total volume of 10.0 mL). Aliquots of the Grignard adduct solution (4.0 mL) were treated with varying aliquots of the 4-toluenesulfonic acid solution (80−320 μL). ^{1}H NMR spectra (400 MHz) of an aliquot of the resulting solution (0.6 mL) mixed with d_8-THF (60 μL) were recorded (relaxation delay of 0.1 s; it was shown separately that the integration stayed constant over a 0.1−10 s range). Spectra were referenced to the 3.58 ppm THF signal. The resolution was enhanced (LB = −1.0 Hz; GB 0.4), and the methyl groups corresponding to **13** (at 1.48 ppm) and the sum of those of **9**−**12** (between 1.275 and 1.375 ppm) were manually integrated.

General Procedure for Kinetic Studies. Hydrogenations were carried out in a 1-L reaction calorimeter (Mettler RC-1). Gas−liquid mass transfer coefficients (k_La) and hydrogen solubilities were determined for a 1:1 mixture of MeOH and THF at various hydrogen gas pressures, reactor fills, and agitation rates. The Grignard adduct substrate solution was prepared as follows. To a solution of **6** (420.0 g; 0.94 mol) in THF (400 mL) was added a solution of 4-fluorophenylmagnesium bromide in THF (0.99 M; 1.30 L; 1.29 mol) between 15 and 25 °C. The resulting solution was stirred for 1 h and then added into methanol (400 mL) which was precooled to −25 °C at such a rate that the temperature was kept below 0 °C. The reaction flask was rinsed with THF (200 mL), and a solution of 4-toluenesulfonic acid monohydrate (357 g; 1.88 mol) in methanol (400 mL) was added in one portion. The resulting solution (total volume adjusted to 3.40 L with methanol) was divided into eight equal portions of 425 mL each. These portions were stored at −15 °C (at which temperature the rearrangement to **19**/**20** does not occur) and warmed to RT immediately prior to use. A portion of the substrate solution and wet Pd/C catalyst was transferred into the reactor. The mixture was degassed repeatedly and then equilibrated under nitrogen at the appropriate temperature. Agitation was stopped, and the headspace was filled with hydrogen to the appropriate pressure. The reaction was started by adjusting the agitation to the desired rate. Heat flow and pressure drop were determined at a rate of 0.5 Hz. At regular intervals samples were taken. These were immediately filtered and diluted with a 100:100:1 mixture of acetonitrile/water/concentrated ammonia. The resulting samples were analyzed by HPLC using a Zorbax Extend C-18 column (5 μm; 4.6 mm × 250 mm; 40 °C) and gradient elution (1.0 mL/min total flow; acetonitrile/0.23 mM ammonia from 60/40 to 90/10) with detection at 210 nm. Low levels of des-F **8** can only be detected by LC−MS using a similar assay and single-ion-monitoring at 455 amu. The concentration−response curves for toluene, **7**, **8**, **14**, and **17** were determined using authentically prepared and/or isolated pure compounds.

Acknowledgment

We thank Anthony Houck, Andrew Newell, Charles Bazaral, and Dr. Anthony King for their expert help in performing hydrogenation experiments.

Received for review October 6, 2005.

OP0501895